Surface Passivation of Sn-Based Wide Band Gap Perovskite Solar Cells Using Functional Molecules

Dhruba B. Khadka[1], Masatoshi Yanagida[1], Roji Sahara[2], and Yasuhiro Shirai[1]

[1]Photovoltaics Materials Group, Global Research Center for Environment and Energy based on Nanomaterials Science (GREEN), National Institute for Materials Science (NIMS), 1-1 Namiki, Tsukuba, Ibaraki 305-0044, Japan

[2]Computational Structural Materials Group, Research Center for Structural Materials, National Institute for Materials Science (NIMS), 1-2-1, Sengen, Tsukuba, Ibaraki, 305-0047 Japan

***Abstract* — Surface passivation with multifunctional molecules is a powerful approach to enhancing the performance and stability of perovskite solar cells (PSCs). This study reports the fabrication of wide-bandgap tin-based perovskite solar cells (WB-Sn-PSCs) with a bandgap of 1.68 eV, achieving a power conversion efficiency of 11.14%. Molecular surface passivation using 4-Fluoro-benzohydrazide (F-BHZ) significantly improves device performance and stability by engineering both the surface and bulk properties of the WB-Sn-HP film. F-BHZ treatment strengthens electrostatic potential and molecular interactions with functional groups, mitigating surface defects and suppressing Sn^{2+} oxidation, as confirmed by theoretical calculations. This work highlights the potential of advanced chemical engineering strategies to optimize non-toxic, lead-free perovskite solar cells, advancing their competitiveness as environmentally friendly photovoltaic solutions.**

I. Introduction

Tandem solar cells (Silicon/perovskite) have progressed by combining narrow bandgap halide perovskites (E_g ~1- 1.3 eV) as bottom cells with wide bandgap Pb-halide perovskites (E_g >1.6 eV) as top cells. [1] However, the toxicity of the lead in the halide perovskite (HP) has been an impugning factor for broader acceptance. Therefore, wide band gap tin perovskites (WB-Sn-HPs) could be one of the best choices for Pb-free Si/perovskite tandem applications.

Few works have been documented for the fabrication of WB-Sn-PSCs using additive engineering.[2] A report by Hu et l. has used an antioxidant additive such as aromatic carboxylic acid molecules in WB-Sn-HP ($FA_{0.75}MA_{0.25}SnI_2Br$) resulting in a PCE of 10.35% with improved device stability.[3] Similarly, Khang and his colleagues obtained a certified record PCE of 11.70% of WB-Sn-PSCs by material engineering using 4-phenylthiosemicarbazide as a functional additive.[4] Cao et al. have reported WB-Sn-PSC using bottom passivation with potassium thiocyanate demonstrating a decent PCE of 11.17% by improving crystallization and interface engineering.[5] Although the knowledge of Pb-PSCs could be utilized in Sn-PSCs,[6], [7], [8], [9] there is still a significant gap in the progress of Sn-based PSCs compared to Pb-PSCs.[10], [11]

In this report, we documented the fabrication of WB-Sn-PSCs (FA, MA, PEA)SnI_2Br) of E_g ~1.68 combined with surface passivation using 4-Fluoro-benzohydrazide (F-BHZ)multifunctional molecule. We achieved among the best PCE of 11.14% with inverted device configuration ITO/PEDOT:PSS/WB-Sn-HP/ICBA/BCP/Ag. The effect of surface passivation of materials properties and device physics have been explored to get insights into the underlying mechanism for the betterment of device performance.

II. Experimental Details

A. Device fabrication

For the fabrication of wide-band gap tin perovskite of composition -$FA_{0.75}MA_{0.10}PEA_{0.15}SnI_2Br$: we prepared 0.85 M of the precursor solution by dissolving FABr (0.75 M), MABr (0.1 M), PEABr (0.15 M), SnI_2 (1 M), SnF2 (0.1 M), Sn powder (5 mg) in the mixture of solvent (dimethylformamide and dimethyl sulfoxide (4:1)) for 2 hours.[12] PEDOT:PSS was used for the hole transport layer.[11], [13], [14] For WB-Sn-HP film deposition, the precursor was spin-coated at 6000 rpm-90 s followed by dripping 0.7 ml of CB at 64^{th} s. Then, these as-grown films were simply placed on a hot plate at 70℃ for 5min. For surface passivation, 4-Fluoro-benzo hydrazide (F-BHZ) precursor solution was spin-coated onto the WB-Sn-HP film at 5000 rpm-50 s and annealed at 70℃-5 min. Then, we deposited ICBA (18 mg/ml-CB) and BCP (2 mg/ml-IPA) by spin coating. Finally, Ag was thermally evaporated. The details have been discussed in our earlier reports.[12]

B. Materials and device characterizations

XRD data were measured using Rigaku Smart Lab, CuKα radiation, λ=1.5405Å. Scanning electron microscopy (SEM) images were collected by a high-resolution scanning electron microscope (SEM) at 5 kV accelerating voltage (Hitachi, S-4800). The absorption and photoluminescence (PL) spectra were measured using a micro-PL spectrometer (HORIBA, LabRamHR-PL NF(UV-NIR). The current density–voltage (J-V) curves were measured under 1 sun with an AM1.5G spectral filter coupled with an MPPT system (Systemhouse Sunrise Corp.). Capacitance spectra (C–f) were collected using an LCR meter (IM3536, Hioki) in the dark.[15], [16]

III. Results and Discussion

To study the effect of surface passivation on WB-Sn-perovskite film with F-BHZ molecule, WB-Sn-PSC, and its device and materials properties have been investigated.

The molecules used for surface passivation are given in Fig. 1a. The F-BHZ molecule possesses higher electron density in the vicinity of hydrazide and carbonyl functionalities showing strong molecular interaction properties. Figure 1b depicts the surface treatment method of WB-Sn-HP film. The molecular interaction of the F-BHZ molecule with Sn-perovskite film has been displayed showing the interaction of Sn with oxygen in the carbonyl group as confirmed by theoretical calculations.[12]

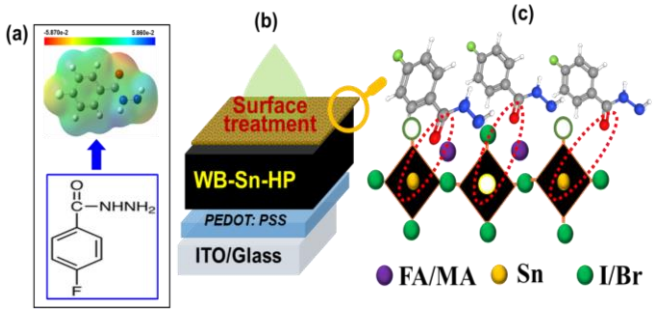

Figure 1. Electrostatic surface potential of 4-Fluoro-benzohydrazide (F-BHZ) (a). Surface passivation of WB-HP with F-BHZ. (c) Schematic of interfacial interaction.

To study the effect of the surface passivation effect on the device, we fabricated WB-Sn-PSC using inverted device configuration of ITO/PEDOT:PSS/WB-Sn-HP/ST(F-BHZ)/ICBA/BCP/Ag as depicted in Figure 2a. Figure 2b shows the current density -voltage characteristics of of WB-Sn-PSCs of control and optimal surface treatment (1 mg/ml- F-BHZ). Inset table 1 displays the figures of merit of respective devices. The control device demonstrated a *PCE* of 7.96% with device parameters; short circuit current density (J_{SC}) ~ 12.58 mAcm^{-2}, pen circuit voltage (V_{OC}) ~ 0.914 V, fill factor (*FF*) ~ 0.692. WB-Sn-PSC with F-BHZ (≤ 1 mg/ml) treated improved *PCE* to ~11.14% with a significant increase in V_{OC} ~ 1.024 V and *FF* ~ 75.7%. This device result is among the best reports on WB-Sn-PSCs.[12] The material growth properties and device characteristics suggest that the compact film morphology, high crystalline quality, modulated surface chemistry, interface energy, and defect passivation.[12], [17] Figure 2c presents the effect of the concentration of F-BHZ on device performance and statistical scenario of device parameters.

Figure 3 a-c shows the surface morphology of control and surface treated WB-Sn-HP films. The WB-HP film treated with F-BHZ displays a well-covered surface with more compact and smoother grains. However, WB-Sn-HP with F-BHZ (Figure 3c) with 2mg/ml grows with unevenly distributed small crystallites, indicating deleterious film quality. This observation aligns with the results of lowers the efficiency of WB-Sn-PSC treated with a higher concentration of F-BHZ (>1.5 mg/ml). This decline is ascribed to the deterioration of film quality stemming from uneven film morphology induced during post-annealing with more concentrated passivated molecules.

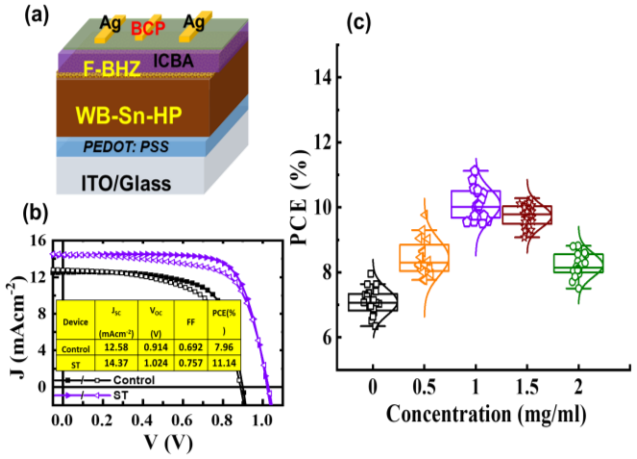

Figure 2. Effect of surface treatment: SEM image of surface treatment-(a) control, (b) PEDAI, (c) PZDI. XRD patterns (d, e) (#-2D phase, δ-non-photoactive perovskite phase and (f) PL spectra of HP film: control, PEDAI, and PZDI treatment.

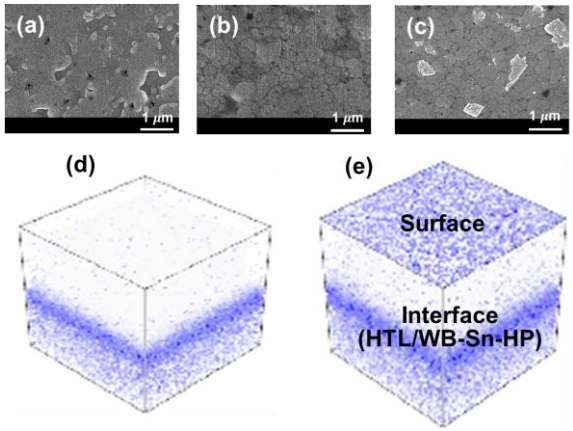

Figure 3. SEM images of WB-Sn-HP films with 4F-BHZ treatment with varying concentrations; (a) control (0 mg), (b) F-BHZ (1 mg/ml), and (c) F-BHZ (2 mg/ml), yellow circles indicate uneven crystallites growth. F-BHZ distribution 3D image reconstructed from the ToF-SIMS depth profiles; d) control and e) F-BHZ treated film.

Figure 3 d,e shows a set of 3D image profiles of F-BHZ molecules using the time-of-flight secondary ion mass spectrometry (ToF-SIMS). The F-BHZ molecule uniformly covers up the surface of the WB-Sn-HP film with a slight diffusion to the bulk through the grain boundary. This supports the suppression of Sn oxidation and defect chemistries in surface-treated WB-Sn-HP film.[12], [17]

Results of this work corroborate the improvement in device performance of WB-PSC with surface passivation of perovskite film using F-BHZ functional molecules.

IV. SUMMARY AND CONCLUSIONS

This report presents a surface method on Sn-based wide band gap perovskite film for the betterment of device efficiency and stability. WB-PSC (1.68 eV) with F-BHZ-treated Sn-perovskite film demonstrated enhanced device efficiency as high as 11.14% compared to the control device of PCE ~ 7.96 %. We found the modulation of the surface chemistry, interface energy by functional molecular bonding, and control of the Sn^{2+} oxidation with uniform distribution of the F-BHZ molecule on WB-Sn-HP film analysis. This work underscores the way for developing efficient and stable WB-Sn-PSC by modulating the defect chemistry with chemical engineering.

ACKNOWLEDGMENT

This work was supported by The Hitachi Global Foundation, Kurata grants #1572.

REFERENCES

[1] R. Lin *et al.*, 'All-perovskite tandem solar cells with 3D/3D bilayer perovskite heterojunction', *Nature*, vol. 620, no. 7976, pp. 994–1000, Aug. 2023, doi: 10.1038/s41586-023-06278-z.

[2] W. J. Jang, H. W. Jang, and S. Y. Kim, 'Recent Advances in Wide Bandgap Perovskite Solar Cells: Focus on Lead-Free Materials for Tandem Structures', *Small Methods*, vol. 8, no. 2, p. 2300207, Feb. 2024, doi: 10.1002/smtd.202300207.

[3] F. Hu *et al.*, 'A vertical antioxidant strategy for high performance wide band gap tin perovskite photovoltaics', *J Mater Chem A Mater*, vol. 11, no. 9, pp. 4579–4586, 2023, doi: 10.1039/D2TA09363D.

[4] P. Pandey *et al.*, '4-Phenylthiosemicarbazide Molecular Additive Engineering for Wide-Bandgap Sn Halide Perovskite Solar Cells with a Record Efficiency Over 12.2%', *Adv Energy Mater*, vol. 14, no. 25, p. 2401188, Jul. 2024, doi: 10.1002/aenm.202401188.

[5] J.-J. Cao *et al.*, 'Multifunctional potassium thiocyanate interlayer for eco-friendly tin perovskite indoor and outdoor photovoltaics', *Chemical Engineering Journal*, vol. 433, p. 133832, Apr. 2022, doi: 10.1016/j.cej.2021.133832.

[6] D. B. Khadka, Y. Shirai, M. Yanagida, and K. Miyano, 'Ammoniated aqueous precursor ink processed copper iodide as hole transport layer for inverted planar perovskite solar cells', *Solar Energy Materials and Solar Cells*, vol. 210, p. 110486, 2020, doi: https://doi.org/10.1016/j.solmat.2020.110486.

[7] D. B. Khadka, Y. Shirai, M. Yanagida, and K. Miyano, 'Unraveling the Impacts Induced by Organic and Inorganic Hole Transport Layers in Inverted Halide Perovskite Solar Cells', *ACS Appl Mater Interfaces*, vol. 11, no. 7, pp. 7055–7065, Feb. 2019, doi: 10.1021/acsami.8b20924.

[8] D. B. Khadka, Y. Shirai, M. Yanagida, T. Noda, and K. Miyano, 'Tailoring the Open-Circuit Voltage Deficit of Wide-Band-Gap Perovskite Solar Cells Using Alkyl Chain-Substituted Fullerene Derivatives', *ACS Appl Mater Interfaces*, vol. 10, no. 26, pp. 22074–22082, 2018, doi: 10.1021/acsami.8b04439.

[9] D. B. Khadka, Y. Shirai, M. Yanagida, J. W. Ryan, and K. Miyano, 'Exploring the effects of interfacial carrier transport layers on device performance and optoelectronic properties of planar perovskite solar cells', *J Mater Chem C Mater*, vol. 5, no. 34, pp. 8819–8827, 2017, doi: 10.1039/C7TC02822A.

[10] D. B. Khadka *et al.*, 'Advancing Efficiency and Stability of Lead, Tin, and Lead/Tin Perovskite Solar Cells: Strategies and Perspectives', *Solar RRL*, vol. 7, no. 21, p. 2300535, Nov. 2023, doi: 10.1002/solr.202300535.

[11] D. B. Khadka, Y. Shirai, M. Yanagida, and K. Miyano, 'Passivation of the Recombination Activities with Rubidium incorporation for Efficient and Stable Sn- HaP Solar Cells', in *2020 47th IEEE Photovoltaic Specialists Conference (PVSC)*, IEEE, Jun. 2020, pp. 0113–0116. doi: 10.1109/PVSC45281.2020.9300783.

[12] D. B. Khadka, Y. Shirai, R. Sahara, M. Yanagida, and K. Miyano, 'Ameliorating Defects in Wide Bandgap Tin Perovskite Solar Cells Using Fluorinated Solvent and Hydrazide', *Small*, pp. 2410048–2410048, Dec. 2024, doi: 10.1002/smll.202410048.

[13] D. B. Khadka, Y. Shirai, M. Yanagida, and K. Miyano, 'Pseudohalide Functional Additives in Tin Halide Perovskite for Efficient and Stable Pb-Free Perovskite Solar Cells', *ACS Appl Energy Mater*, vol. 4, no. 11, pp. 12819–12826, Nov. 2021, doi: 10.1021/acsaem.1c02496.

[14] D. B. Khadka, Y. Shirai, M. Yanagida, T. Masuda, and K. Miyano, 'Enhancement in efficiency and optoelectronic quality of perovskite thin films annealed in MACl vapor', *Sustain Energy Fuels*, vol. 1, no. 4, pp. 755–766, 2017, doi: 10.1039/C7SE00033B.

[15] D. B. Khadka *et al.*, 'Defect passivation in methylammonium/bromine free inverted perovskite solar cells using charge-modulated molecular bonding', *Nat Commun*, vol. 15, no. 1, p. 882, Jan. 2024, doi: 10.1038/s41467-024-45228-9.

[16] D. B. Khadka, Y. Shirai, M. Yanagida, T. Tadano, and K. Miyano, 'Interfacial Embedding for High-Efficiency and Stable Methylammonium-Free Perovskite Solar Cells with Fluoroarene Hydrazine', *Adv Energy Mater*, vol. 12, no. 38, p. 2202029, Oct. 2022, doi: 10.1002/aenm.202202029.

[17] D. B. Khadka, Y. Shirai, M. Yanagida, T. Tadano, and K. Miyano, 'Alleviating Defect and Oxidation in Tin Perovskite Solar Cells Using a Bidentate Ligand', *Chemistry of Materials*, vol. 35, no. 11, pp. 4250–4258, Jun. 2023, doi: 10.1021/acs.chemmater.3c00243.